Development of Drive Control Strategy for Front-and-Rear-Motor-Drive Electric Vehicle (FRMDEV)

Binbin Sun, Bo Li, Yongjun Wang, Wenqing Ge & Song Gao*

School of Transportation and Vehicle Engineering, Shandong University of Technology, 255049, Zibo, Shandong, China
*E-mail: gaos546@126.com

Abstract. In order to achieve both high-efficiency drive and low-jerk mode switch in FRMDEVs, a drive control strategy is proposed, consisting of top-layer torque distribution aimed at optimal efficiency and low-layer coordination control improving mode-switch jerk. First, with the use of the off-line particle swarm optimization algorithm (PSOA), the optimal switching boundary between single-motor-drive mode (SMDM) and dual-motor drive mode (DMDM) was modelled and a real-time torque distribution model based on the radial basis function (RBF) was created to achieve the optimal torque distribution. Then, referring to the dynamic characteristics of mode switch tested on a dual-motor test bench, a torque coordination strategy by controlling the variation rate of the torque distribution coefficient during the mode-switch process was developed. Finally, based on a hardware-in-loop (HIL) test platform and an FRMDEV, the proposed drive control strategy was verified. The test results show that both drive economy and comfort were improved significantly by the use of the developed drive control strategy.

Keywords: *front-and-rear-motor-drive electric vehicle; drive control strategy; torque distribution; torque coordination control.*

1 Introduction

To relieve the pressure caused by the fossil energy crisis and environmental pollution, the development of electric vehicles (EVs) has attracted a large amount of attention from the automobile industry owing to the abundant ways of generating electricity with low or no emission [1,2]. FRMDEVs with independent drive motors on the front and the rear axle offer great flexibility for performance optimization [3,4]. Plentiful achievements have been obtained in the improvement of dynamic, stability and safety performance of FRMDEVs [5-7]. Torque distribution between front and rear motors aimed at both high-efficiency drive and comfortable mode switch is of great importance but has still been insufficiently studied.

Currently, rule algorithms and optimization algorithms are the most commonly used methods to develop torque distribution strategies with the goal of economy

Received February 4th, 2018, Revised July 30th, 2018, Accepted for publication November 30th, 2018.
 ISSN: 2337-5779, DOI: 10.5614/j.eng.technol.sci.2018.50.5.9

optimization [8-10]. The former method can be applied in engineering but is unable to achieve optimal drive efficiency. The latter method can improve drive economy effectively but with bad real-time performance. Consequently, to create a torque distribution strategy that can balance both efficiency optimization and engineering application is of great importance. Furthermore, different from mode-switch jerk in hybrid electric vehicles, which is mainly caused by the response difference between the engine and the motor [11-13], the response difference between the front motor and the rear motor of FRMDEVs is unobservable [14]. Consequently, it is still unclear whether the mode-switch jerk of FRMEDVs is significant. More importantly, if it is significant, the coordination control strategy is still unconfirmed.

Given the above analysis, in this study, a drive control strategy for FRMDEVs that can balance economy and mode-switch comfort was investigated. First, a top-layer torque distribution strategy aimed at optimal driving efficiency was formulated based on the response surface method. Then, mode-switch jerk was tested and a low-layer torque coordination control strategy was developed. Finally, the vehicle control strategy of an FRMDEV was modeled based on Simulink/MotoHawk to verify the drive control strategy. Owing to the multi-objective control strategy developed in this study, both drive economy and mode-switch jerk of the FRMDEV were improved significantly, which lays a foundation for the development of a new drive control method and the improvement of FRMDEV performance.

2 The Top-Layer Torque Distribution Strategy

In this section, firstly, the characteristics of the FRMDEV are specified. Secondly, the loss caused by the non-work motor is analyzed based on a test that was conducted. Thirdly, a fitness function developed for PSO is created based on THE HALTON sequence method. Finally, the top-layer torque distribution strategy is developed and verified.

2.1 Configuration of the FRMDEV

In the FRMDEV shown in Figure 1, the powertrain system consists of a permanent magnet synchronous motor (PMSM) in the front, an induction motor (IM) in the rear, and two one-speed transmissions on the front and the rear axle. A CAN bus is used to achieve the communications between the vehicle control unit (VCU) and the front motor control unit (MCU), the rear MCU and the battery management system (BMS). For any normal driving operation there are three VCU modes to choose from, i.e. single-IM-drive mode (mode 1), single-PMSM-drive mode (mode 2) and dual-motor-drive mode (mode 3).

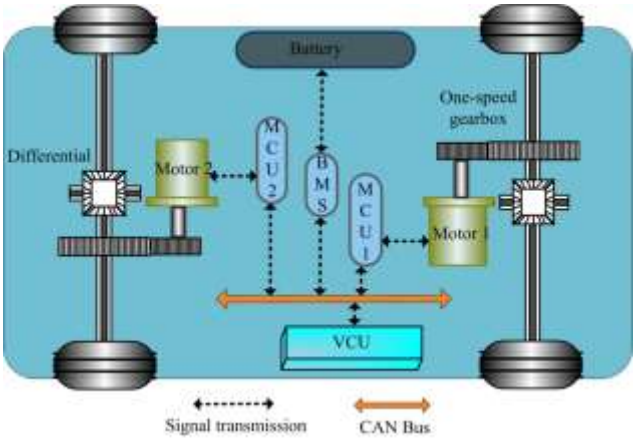

Figure 1 Electric vehicle driven by front and rear motors.

2.2 Losses Caused by Motored IM and PMSM

For the torque distribution strategy aimed at optimal driving efficiency of the dual-motor powertrain system, the effect of the non-work motor under single-motor-drive mode needs to be dealt with as there still exists resistance in the motored motor. As shown in Table 1, the resistances caused by the motored IM and PMSM increase with the increase of the motored speed.

Table 1 Resistances of motored PMSM and IM.

Motored speed/r.min^{-1}	Resistances of motored motor/N.m	
	PMSM	IM
500	2.3	1.7
1000	3.0	2.1
1500	3.5	2.6
2000	4.1	3.0
2500	4.6	3.6
3000	5.3	4.0

Taking the operation of T_d (drive torque required by driver) at 5 N.m, N (motor speed) at 1500 r.min^{-1} as an example (see Table 2), the actual power losses of the dual-motor system were tested under three modes. As for mode 1, if the effect of the non-work PMSM is not taken into account, the driving loss caused by the IM is about 120 W. However, for the given driving operation, the IM actually needs to output extra torque (2.6 N.m) to cover the drag caused by the motored PMSM, which is equivalent to vehicle resistance. Consequently, the tested power loss is 151 W rather than 120 W, which also applies to mode 2. As

for mode 3, T_d is equally distributed to IM and PMSM. Consequently, the ideal system power loss is equal to the actual one, as there is no motored loss in the dual motors.

Table 2 Power losses under different test modes.

Items	Mode 1	Mode 2	Mode 3
Required torque/N.m	5	5	5
Actual torque/N.m	7.6	8.5	5
Ideal system power loss/W	120	120	120
Actual system power loss/W	151	163	120

Note: the ideal system power loss designates the driving loss of the dual-motor system without considering the non-work motor, while the actual system power loss takes the effect of the non-work motor into consideration under the SMDM.

2.3 Design of Fitness Function

Given the above analysis, it can be confirmed that when a PSOA [15] is designed aimed at minimal system power loss, the effect of the non-work motor should be dealt with. Consequently, as shown in Figure 2, for any of the random drive operations designed based on the HALTON sequence method, the fitness function of system power loss under this operation can be expressed as follows.

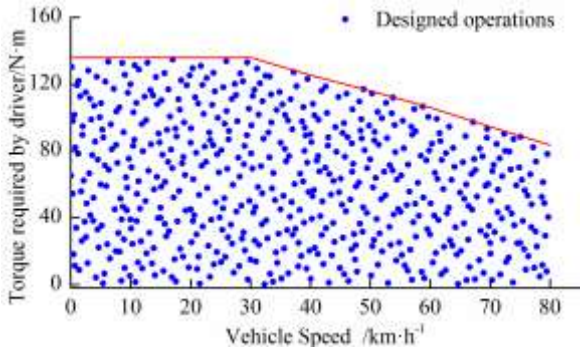

Figure 2 Random drive operations designed by HALTON sequence.

Taking operation number i as an example, for mode 3 ($0 < \beta < 1$), the fitness function can be designed as follows:

$$F_{it}(\beta)=P_{sm\_i}(\beta)+P_{im\_i}(\beta) \tag{1}$$

where $F_{it}(\beta)$ is the fitness function of PSOA. β is the torque distribution coefficient, which is defined as the ratio between the torque distributed to IM and the total one required by driver. $P_{sm\_i}(\beta)$ and $P_{im\_i}(\beta)$ are the power losses caused by PMSM and IM. Both can be modeled as follows:

$$\begin{cases} P_{sm\_i}(\beta)=P_{pub} & \text{if:}\ (1-\beta)T_{di}>1.25T_{se} \\ P_{sm\_i}(\beta)=P_{ls}\left(T_{di}(1-\beta),V_i\right) & \text{if:}\ (1-\beta)T_{di}\leqslant 1.25T_{se} \\ P_{im\_i}(\beta)=P_{pub} & \text{if:}\ \beta T_{di}>1.25T_{ie} \\ P_{im\_i}(\beta)=P_{ls}\left(T_{di}(\beta),V_i\right) & \text{if:}\ \beta T_{di}\leqslant 1.25T_{ie} \end{cases} \quad (2)$$

where T_{di} is the torque required by the driver under operation number *i*. P_{ls} is the function for the loss caused by the motor, which can be confirmed based on the motor loss tested under different operations. P_{pub} is a penalty function designed to prevent too much torque being distributed to one motor. V_i is the vehicle speed under operation number *i*. T_{se} and T_{ie} designate the nominal torque of the PMSM and IM, respectively.

For mode 1 (β = 1), the additional power loss caused by the PMSM should be dealt with. The fitness function under this mode can be expressed as follows:

$$F_{it}(\beta)=P_{im\_i}(\beta)+P_{sm\_mt} \quad (3)$$

$$T_{di\_c}=T_{di}+T_{sm\_mt} \quad (4)$$

where T_{di_c} is the actual torque output from the drive motor. T_{sm_mt} and P_{sm_mt} are the equivalent torque and power caused by the motored PMSM.

For mode 2 (β = 0), the additional power loss caused by the IM should be dealt with. The fitness function under this mode can be expressed as follows:

$$F_{it}(\beta)=P_{sm\_i}(\beta)+P_{im\_mt} \quad (5)$$

$$T_{di\_c}=T_{di}+T_{im\_mt} \quad (6)$$

where T_{im_mt} and P_{im_mt} are the equivalent torque and power caused by the motored IM.

2.4 Predictive Model of the Optimal Torque Distribution Strategy

With the use of the off-line PSOA, the optimization results were confirmed as shown in Figure 3. A predictive model was created as shown in Eq.(7). For low load operations, the single-PMSM-drive mode is preferred ($\beta = 0$) to achieve optimal driving efficiency, while under middle to high load conditions, the DMDM takes priority over the SMDM to balance both economy and dynamic performance of the FRMDEV. Furthermore, the single-IM-drive mode is not allowed due to the lower driving efficiency of the IM under low load operations.

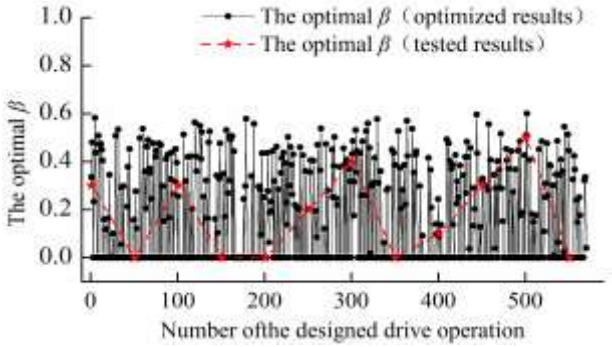

Figure 3 The optimal β based on PSOA.

The test results were achieved based on the dual-motor test platform shown in Figure 5. Based on the optimization results of β shown in Figure 3, the optimal torque distribution model was developed based on the radial basis function (RBF). Moreover, both the modeling precision and the predictive accuracy were calculated. The coefficient of determination (R^2) and the root-mean-square error (RMSE) were 0.986 and 0.017 respectively, which indicates that the torque-distribution-prediction model has high modeling precision. The $RMSE_{PRESS}$ (predicted residual sum of squares, PRESS) was about 0.018, which means that the developed torque distribution model can be used to predict the optimal torque distribution coefficient according to vehicle speed and required drive torque.

$$\begin{cases} \hat{T}_{sw} = \sum_{i=1}^{10} w_{i\_T}\phi_{i\_T} + \sigma_T \\ \phi_{i\_\beta} = \exp\left(-\dfrac{\left\|\vec{x} - \overrightarrow{c_{i\_T}}\right\|^2}{2b_{i\_T}{}^2}\right) \\ \hat{\beta} = \sum_{i=1}^{10} w_{i\_\beta}\phi_{i\_\beta} + \sigma_\beta \\ \phi_{i\_\beta} = \exp\left(-\dfrac{\left\|\vec{x} - \overrightarrow{c_{i\_\beta}}\right\|^2}{2b_{i\_\beta}{}^2}\right) \end{cases} \tag{7}$$

where $\hat{T}_{sw}$ is the predictive mode-switch boundary, which is a function of vehicle speed. $\hat{\beta}$ is the predictive torque distribution coefficient. w_i is the

weight coefficient of RBF, as shown in Tables 3 and 4. ϕ_i is the Gauss function. σ is the regularization parameter. $\vec{x}$ means the input of RBF. $\vec{c_i}$ is the central vector of RBF nodes as shown Tables 3 and 4. b_i is the base width.

Table 3 Parameters of the predictive mode-switch boundary based on RBF.

Number	w_{i_T}	V_{i_T}
1	6.23	5.79
2	9.76	26.34
3	-1.47	50.89
4	0.856	77.21

Table 4 Parameters of the predictive torque distribution model based on RBF.

Number	w_{i_β}	V_{i_β}	T_{di_β}
1	4.31	62.19	57.22
2	1.13	67.19	97.22
3	-1.76	79.06	48.89
…	…	…	…
9	-3.47	73.44	68.89
10	-3.17	31.33	101.86

Furthermore, as shown in Figure 4, taking the cross-section of the predictive model (V is 41.56 km.h^{-1} and T_d is 61.77 N.m) as an example, in this cross-section almost all of the sample points used for developing the predictive model are within the confidence interval (95%). Generally, the above discussion validates the feasibility of the developed model.

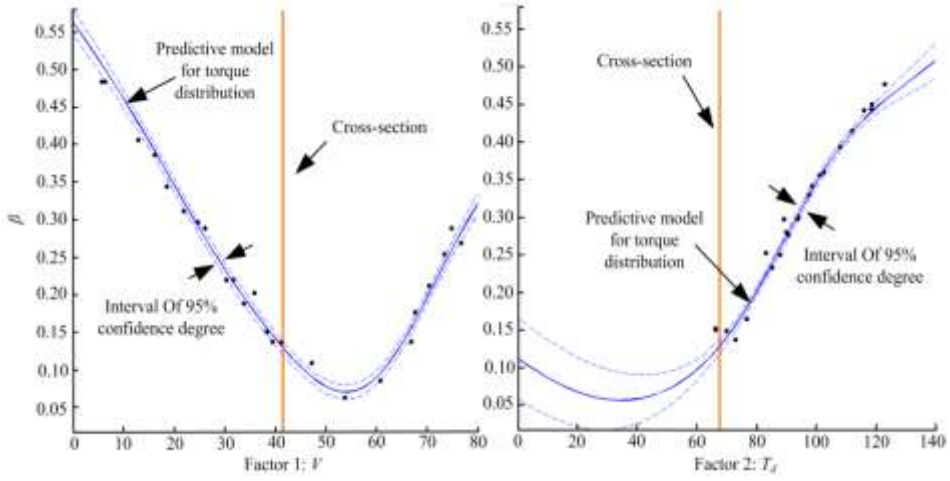

Figure 4 Predictive results of the sample operation V = 41.56 km.h^{-1} and T_d = 61.77 N.m.

3 The Low-Layer Torque Coordination Control Strategy

In this section, to develop a torque coordination control strategy aimed at improving mode-switch jerk, first, jerk during different switching modes was tested and analyzed. Then, the coordination control strategy was developed by controlling the changing rate of the torque distribution coefficient.

3.1 Mode-switch Jerk

As the theoretical mode-switch jerk model in Eq. (8) shows, the changing rate of the total torque output from the front and the rear transmission leads to mode-switch jerk.

$$\begin{cases} j = \dfrac{1}{R\delta m}\dfrac{d\left(T_{im}i_f\eta_{tf} + T_{sm}i_r\eta_{tr}\right)}{dt} \\ T_{im} = \beta T_d \\ T_{sm} = \left(1-\beta\right)T_d \end{cases} \tag{8}$$

where j is the mode-switch jerk. R is the vehicle wheel radius. i_f and i_r are the ratios of the front and rear transmission system. m is the vehicle mass. δ is the mass conversion factor.

Theoretically, there is little difference between the torque response times of the front and rear motors [14]. Consequently, for the FRMDEV discussed in this paper, since it is equipped with the same transmission on the front and rear axles, the theoretical jerk under various switch modes is close to 0 $m.s^{-3}$. However, affected by the actual response difference between the front and rear motors, the mode-switch jerk during various switching processes is considerable. Taking the given test condition (T_d = 50 N.n, N = 500 $r.min^{-1}$) as an example, based on the dual-motor test platform shown Figure 5, the mode-switch jerk was tested under various switching modes.

As shown in Figure 6, taking the switch comfort problem from the SMDM to the SMDM as an example, during the switching process from motor 1 to motor 2, the torque increase of motor 1 as region A shown in Figure 6(b) is lower than the torque decrease of motor 2 as region B shown in Figure 6(b), and the obvious difference of torque response between the two motors actually results in the switching jerk shown in Figure 6(a). Furthermore, as the tested mode-switch jerk under various operations in Table 5 shows, the switch comfort problem from the SMDM to the SMDM is more serious than that from the DMDM to the SMDM. Given the above analysis, different from the theoretical

switch-jerk model, torque coordination control is required to optimize the switch jerk of the FRMDEV under actual operations.

Figure 5 The developed dual-motor test platform: (1) control unit of motor 1; (2) motor 1; (3) host computer; (4) electric dynamometer; (5) industrial personal computer; (6) gearbox; (7) motor 2; (8) control unit of motor 2.

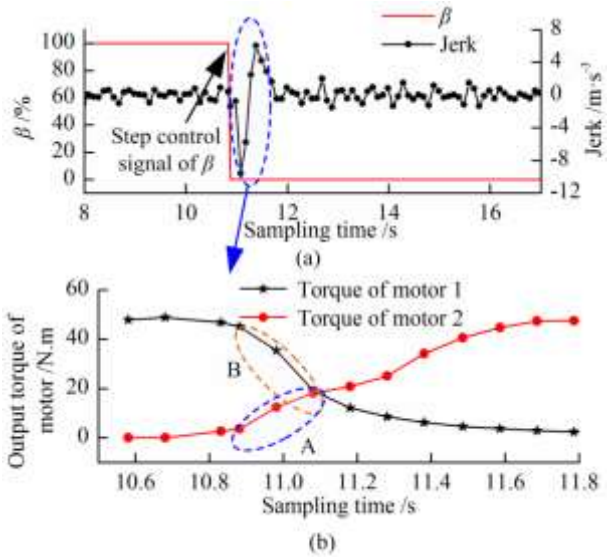

Figure 6 The tested mode-switch jerk based on the dual-motor test platform: (a) the mode-switch jerk, (b) the characteristics of the torque responses.

Table 5 Mode-switch Jerk under various test operations.

Switch mode	Test operation		Jerk
	N/r.min^{-1}	T_d/N.m	j/m.s^{-3}
SMDM to SMDM	1000	70	12.35
SMDM to SMDM	3000	40	7.42
SMDM to DMDM	1000	70	8.04
SMDM to DMDM	3000	40	5.63
DMDM to SMDM	1000	70	7.89
DMDM to SMDM	3000	40	5.42

3.2 Torque Coordination Control Strategy

To reduce the mode-switch jerk caused by the significant response difference between motor and engine in hybrid electric vehicles, complex control methods have been developed [11-13]. However, different from hybrid electric vehicles, for the FRMDEV as shown in Figure 5, the difference of dynamic response to step control signal (β is from 0 to 1) between motor 1 and motor 2 results in switch jerk. To optimize the mode-switch jerk, the transfer function in Eq. (9) is proposed, which controls the changing rate of the single control variable (β):

$$H(s)=\frac{1}{0.1s+1} \tag{9}$$

4 Verification

A hardware-in-loop test platform and a test vehicle was developed to verify the drive control strategy proposed in this paper. The test results were analyzed.

4.1 Hardware-in-loop Test

The software part of the vehicle control strategy of the FRMDEV was developed based on Simulink/MotoHawk, as shown in Figure 7. The control strategy mainly consists of the following parts: (1) a time-triggered module developed for setting the sampling step length of the control strategy; (2) an engineering definition module designed for defining the hardware resource, the communication protocol and the program compiling, etc.; (3) a signal input module developed for setting the CAN bus and sensor signals; (4) a vehicle control strategy module, including the power-on and power-off control, accessory control, drive control, etc.; (5) a signal output module designed for outputting the control, status and alarm signals.

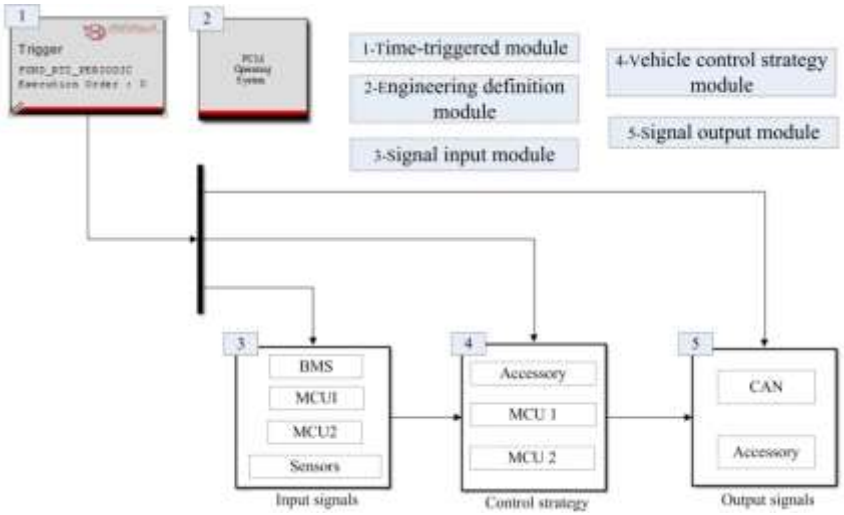

Figure 7 The frame of the vehicle control strategy.

As shown in Figure 8, referring to the start/stop, gear and pedal signals etc., the drive control module includes the top-layer torque distribution strategy aimed at optimal drive efficiency and the low-layer torque coordination control strategy designed for optimizing mode-switch jerk developed to output the control signals for the front and rear motors.

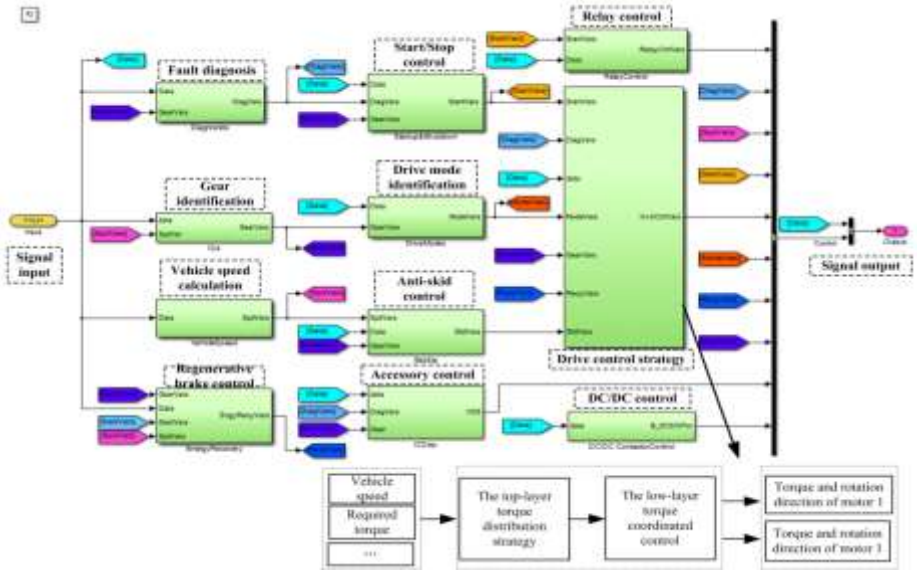

Figure 8 The vehicle control strategy of FRMDEV.

To simplify the code development of the vehicle control strategy, a hardware-in-loop test platform was developed as shown in Figure 9. RTS is short for real-time simulator, which is used to run the FRMDEV dynamic model and simulate the working condition of the FRMDEV. The VCU was used to download the code of the control strategy developed on the host computer and achieve vehicle control.

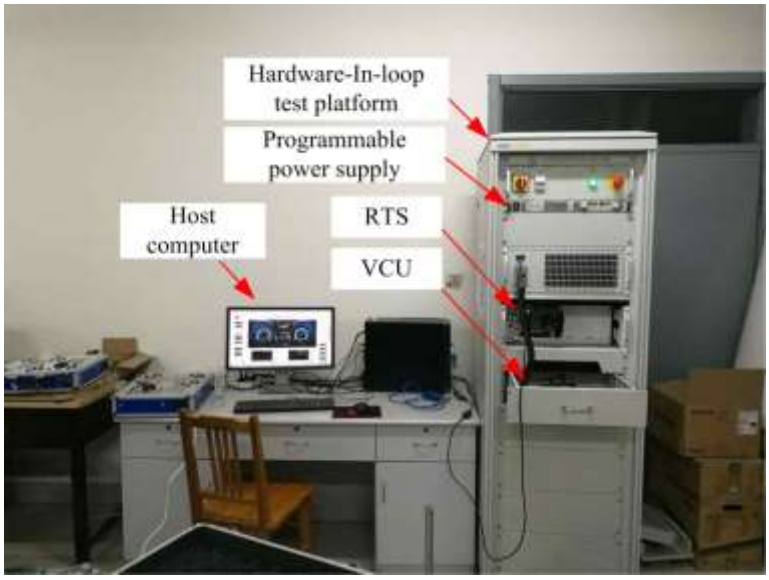

Figure 9 The hardware-in-loop test platform.

Based on the hardware-in-loop test platform, the drive control strategy developed above was tested under the NEDC drive cycle, as shown in Figure 10(a). Referring to the test result shown in Figure 10, the following can be concluded.

First of all, as shown in Figure 10(a), the deviation between the actual speed and the desired speed was very small, which indicates that the developed vehicle control strategy is feasible. Secondly, as shown in Figure 10(b), based on the predictive torque distribution strategy modeled in the form of RBF, the FRMDEV can operate under the single-PMSM-drive mode and the DMDM for urban and suburban conditions respectively, which means the predictive torque distribution strategy can balance both real-time performance and energy-efficiency optimality. Furthermore, as shown in Figure 10(c), compared with the original EV driven by a single motor on the front shaft, under the NEDC drive cycle, lower energy consumption was achieved owing to the top-layer

predictive torque distribution strategy. The energy consumption was reduced by 6.51% compared with the original EV.

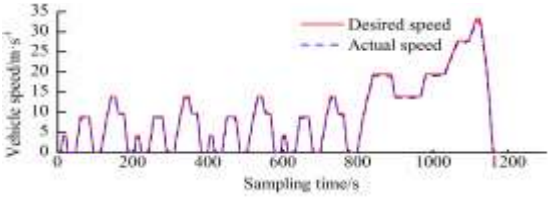

(a) Characteristics of vehicle speed

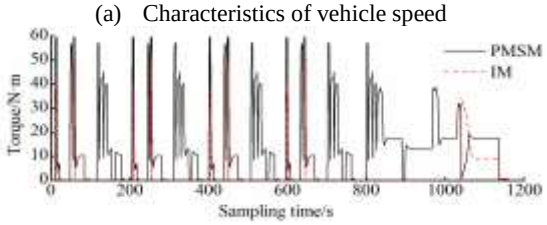

(b) Characteristics of motor torque

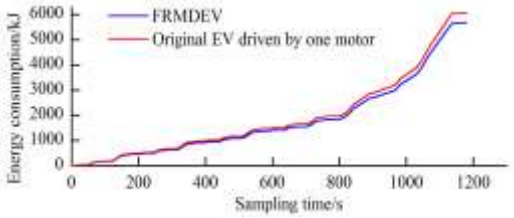

(c) Characteristics of energy consumption

Figure 10 The hardware-in-loop test result.

As shown in Table 6, in comparison with the FMDEV, the ratio coefficient of the FRMDEV operating under high-efficiency condition (＞ 90%) increased 124.8%, while the ratio coefficient of the FRMDEV operating under low-efficiency condition (＜ 80%) decreased 76.7%. The economy of the FRMDEV was improved significantly based on the predictive torque distribution strategy proposed in this paper.

Table 6 Drive Efficiency of FRMDEV and FMDEV.

Items		**The range of efficiency**				**Average efficiency**
		＞ 90%	**90%-85%**	**85%-80%**	**＜ 80%**	
Ratio coefficient/%	FRMDEV	37.36	30.52	19.23	12.89	81.17
	FMDEV	16.62	20.71	7.34	55.33	76.21

4.2 Vehicle Test

As shown in Figure 11, an FRMDEV was developed to test the developed drive control strategy. With the use of CANape, the statuses of the FRMDEV, front motor, rear motor and battery were obtained. As the test results in Figure 12 show, for the given acceleration and cruise conditions, the developed drive control strategy was able to achieve the single-PMSM-drive under low load conditions and the dual-motor-drive mode under high load conditions (acceleration conditions). Consequently, both economic optimization under low load conditions and dynamic satisfaction under high load conditions were achieved.

Figure 11 The test FRMDEV.

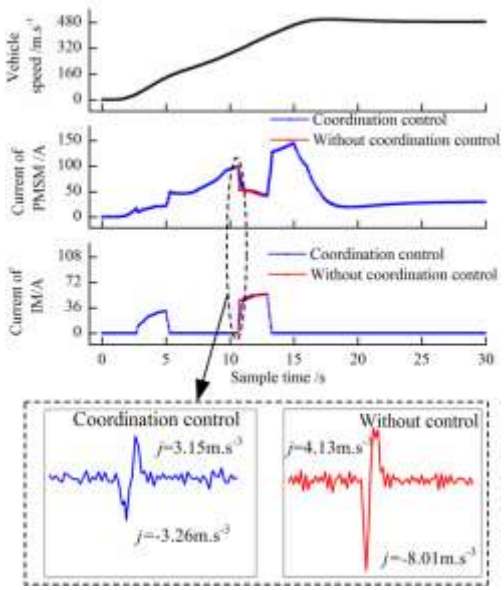

Figure 12 The test results based on the FRMDEV.

Furthermore, compared with the drive control strategy without low-layer torque coordination control strategy, the developed drive control strategy could achieve significant improvement of mode-switch jerk. As shown in Figure 12, for the given test operation, the mode-switch jerk was reduced by 59.3% owing to the use of the low-layer torque coordination control strategy.

5 Conclusions

In this study, a drive control strategy for an FRMDEV that can balance both economy and mode-switch comfort was investigated. When the FRMDEV operates under the single-motor-drive mode, the motored motor actually wastes driving energy. Consequently, an optimization program aimed at optimal driving efficiency needs to take the motored loss into account. In the mode-switch process, by controlling the changing rate of the torque distribution coefficient, mode-switch jerk caused by the dynamic response difference of the motor intervening drive and the motor exiting drive can be reduced significantly. The proposed drive control strategy for the FRMDEV consists of a top-layer torque distribution aimed at economy optimization and low-layer torque coordination with the goal of jerk optimization. It was proven to be effective in improving the driving performance of the FRMDEV.

The obtained conclusions are as follows:

1) Commonly, torque distribution models based on a rule algorithm have strong real-time performance but with low drive efficiency. In contrast, torque distribution models based on an optimization algorithm can achieve higher drive efficiency but with poor real-time ability. The torque distribution model based on the response surface method and RBF proposed in this paper was verified to be able to balance both drive efficiency and real-time ability, which provides a new method for the development of drive control.

2) The non-work motor under SMDM showed significant influence on system loss. A fitness function designed for optimization of the torque distribution should consider this effect. Compared with the original front-motor-drive EV, the proposed torque distribution strategy reduced energy consumption by 6.51% under the NEDC drive cycle.

3) Based on the analysis of the test result of mode-switch jerk, a torque coordination strategy controlling the variation rate of the torque distribution coefficient was developed and verified. Mode-switch jerk was reduced by 59.3%. The comfort of the FRMDEV was improved significantly based on the coordination control strategy proposed in this paper.

Acknowledgments

This work was supported by the National Natural Science Foundation Project of China (51805301), the Scientific Research Project of Universities in Shandong (J18KA021), the Zibo City-Shandong University of Technology Cooperative Projects (2017ZBXC165), and the Natural Science Foundation of Shandong Province (ZR2018LF009).

Reference

[1] Dang, S., Odonde, A., Mirza, T., Dissanayake, C. & Burns, R., *Sustainable Energy Management: An Analysis Report of the Impacts of Electric Vehicles*, in 2014 14th International Conference on Environment and Electrical Engineering, pp. 318-322, 2014.

[2] Skarka, W., *Reducing the Energy Consumption of Electric Vehicles*, in 22nd ISPE Inc. International Conference on Concurrent Engineering, pp. 500-509, 2015.

[3] Sun, B., Gao, S., Wu, Z. & Li, J., *Parameters Design and Economy Study of an Electric Vehicle with Powertrain Systems in Front and Rear Axle*, International Journal of Engineering Transactions A: Basics**, 29**(4), pp. 454-463, 2016.

[4] Sun, B., Gao, S. & Ma, C., *Mathematical Methods Applied to Economy Optimization of an Electric Vehicle with Distributed Power Train System*, Mathematical Problems in Engineering, pp. 1-14, 2016.

[5] Kang, J., Yoo, J. & Yi, K., *Driving Control Algorithm for Maneuverability, Lateral Stability, and Rollover Prevention of 4WD Electric Vehicles with Independently Driven Front and Rear Wheels*, IEEE Transaction on Vehicular Technology, **59**(10), pp. 3919-3933, 2012.

[6] Mutoh, N., Kato, T. & Murakami, K., *Front-and-Rear-Wheel-Independent-Drive-Type Electric Vehicle（FRID EV）Taking the Lead for Next Generation ECO-Vehicles*, SAE Paper, 2011-39-7.

[7] Guo, H., He, H. & Sun, F., *A Combined Cooperative Braking Model with a Predictive Control Strategy in an Electric Vehicle*, Energies, **6**, pp. 6455-6475, 2013.

[8] Marco, S., Gianfranco, R. & Ivan, A., *Analysis of a Rule-based Control Strategy for On-board Energy Management of Series Hybrid Vehicles*, Control Engineering Practice, St. Louis, MO, United States, June 10-12, 2011, 19, pp. 1433-1441.

[9] Li, Q., Chen, W. & Li, Y., *Energy Management Strategy for Fuel Cell/Battery/Ultra Capacitor Hybrid Vehicle Based on Fuzzy Logic*, International Journal of Electrical Power and Energy Systems**, 43**(1), pp. 514-525, 2012.

[10] Lorenzo, S., Simona, O. & Giorgio, R., *A Comparative Analysis of Energy Management Strategies for Hybrid Electric Vehicles*, Journal of Dynamic Systems, Measurement and Control, 2011, **133**(3), pp. 1-9, 2011.

[11] Kim S., Park J., Hong J., Lee M. & Sim H., *Transient Control Strategy of Hybrid Electric Vehicle during Mode Change*, SAE Paper: 2009-01-0228.

[12] Wang, L., Zhang, Y., Shu, J. & Yin, Ch., *Mode Transition Control for Series-parallel Hybrid Electric Bus Using Fuzzy Adaptive Sliding Mode Approach*, Journal of Mechanical Engineering, **48**(14), pp. 119-127, 2012.

[13] Zhang, J. & Zhou, Y., *A Study on Mode Switching Smoothly on Hybrid Electric Vehicle Based on CVT*, International Conference on Remote Sensing, Environment and Transportation Engineering. Piscataway, USA: IEEE, pp. 972-975, 2011.

[14] Wang, H., *Study on the Torque Coordination Algorithm for Driving Mode-Transition of Parallel Hybrid Electric Bus*, Master of Engineering, Jilin University, China, 2013.

[15] Jam, S., Shahbahrami, A. &Ziyabari, S.H.S., *Parallel Implementation of Particle Swarm Optimization Variants Using Graphics Processing Unit Platform*, International Journal of Engineering Transactions A: Basics, **30**(1), pp. 48-56, 2017.